Status of hybrid trigger system of the Telescope Array experiment

H. TOKUNO[1,2], R. ISHIMORI[1], T.NONAKA[3], T.FUJII[4], D.IKEDA[3], S. KITAMURA[1], S.OGIO[4], J.SMITH[5], A.TAKETA[3], Y. TSUNESADA[1], Y.YAMAKAWA[3], FOR THE TELESCOPE ARRAY COLLABORATION
[1]*Graduate School of Science and Engineering, Tokyo Institute of Technology, Meguro, Tokyo 152-8551, Japan*
[2]*Interactive Research Center of Science, Graduate School of Science and Engineering, Tokyo Institute of Technology, Meguro, Tokyo 152-8551, Japan*
[3]*Institute for Cosmic Ray Research, The University of Tokyo, Kashiwa, Chiba 277-8582, Japan*
[4]*Department of Physics and High Energy Astrophysics Institute, University of Utah, Salt lake city, Utah 84112, USA*
[5]*Graduate School of Science, Osaka City University, Sumiyoshi, Osaka 558-8585, Japan*
htokuno@cr.phys.titech.ac.jp

Abstract: The Telescope Array consists of a surface detector (SD) array and three fluorescence detector (FD) stations. Since May 2008, the SD array and the FDs have been operating with independent triggers. Below $10^{18.5}$ eV, adding SD information to the FD analysis improves reconstruction accuracy greatly, however these showers do not always trigger the SD array. In order to obtain this information, we have installed an external trigger of the SD array from the FD called the hybrid trigger. Installation of the hybrid trigger was finished in October 2010, and additional SD information is recorded during FD observation since that time. In this paper, we introduce the scheme of our hybrid trigger system and its operation status.

Keywords: Ultra high energy cosmic rays, air Fluorescence detector, data acquisition

1 Introduction

Located in the west desert of Utah, USA, the Telescope Array (TA) experiment has been observing ultra-high energy cosmic rays (UHECRs) since May 2008 [1, 2]. TA consists of an array of 507 surface detectors (SDs) and three fluorescence detector (FD) stations. Our preliminary result and other results [3, 4, 5] suggest that the dominant component of the cosmic rays at $10^{18.5}$ eV is lighter nuclei. On the other hand, the previous experimental results (e.g. [6, 7]) suggest that the composition is heavier at 10^{16} eV. If these results are correct, cosmic ray composition must transition between 10^{16} eV to $10^{18.5}$ ([8, 9, 10]). This transition may be caused by differences in their origin or propagation processes. To study their origin and these processes, we need a more precise determination of the energy spectrum and the composition in this energy range.

Full SD array operation started in May 2008. The array covers an area of about 700 km^2; it is divided into three sub-arrays shown in figure 1. Each sub-array has a central control PC at the sub-array's control and communications tower that forms the trigger for that sub-array, and the PC at the Smelter Knolls (SK) tower coordinates the other two PCs to make a trigger decision on the sub-array boundaries. Before the installation of the hybrid trigger, the SD array operated with its own trigger. Three FD stations are placed

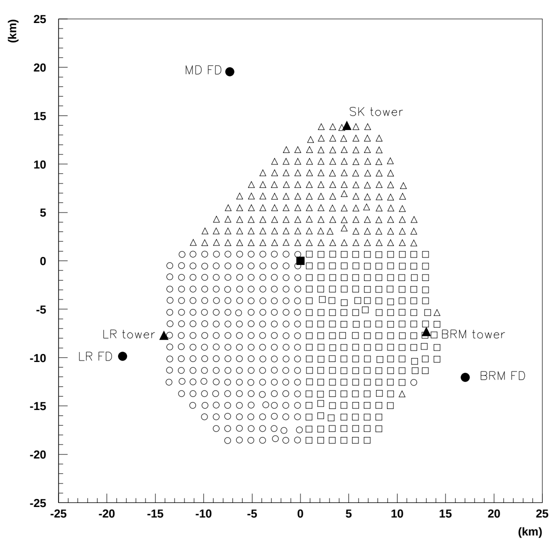

Figure 1: The detector position of the telescope array experiment. Open squares,Open triangles,Open circles: surface detectors in BRM, in SK, and in LR sub-array respectively. Filled circles: the telescope stations. Filled square: the central laser facility. Filled triangles: the SD control tower.

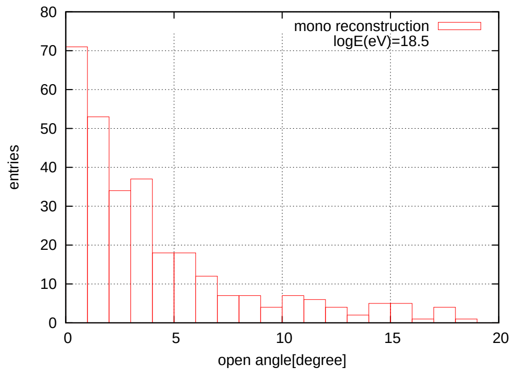

Figure 2: The simulation results of accuracy of arrival direction determination from FD mono reconstruction at the primary energy $10^{18.5}$ eV.

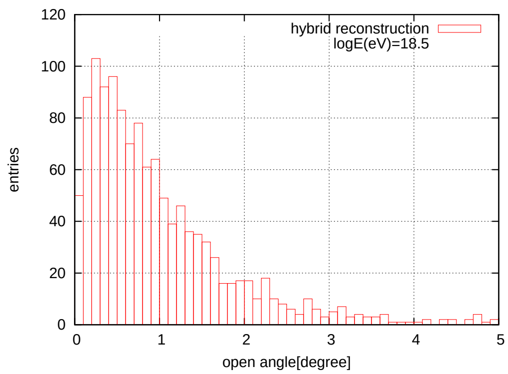

Figure 3: The simulation results of accuracy of arrival direction determination from FD with one SD reconstruction at the primary energy $10^{18.5}$ eV.

around the SD array as shown in figure 1. Each FD station run with an independent trigger during clear moonless nights.

At energies below $10^{18.5}$ eV, adding timing and location information from even one SD can improve the FD reconstruction accuracy of extensive air shower (EAS) parameters (e.g. arrival direction, primary energy, and Xmax) greatly [12]. For example, figure 2 and figure 3 show the results of reconstructing the arrival direction of simulated $10^{18.5}$ eV EAS using information from only one FD (FD mono) and from one FD with additional data from one SD. Plotted is the difference in angle between the simulated and reconstructed EAS.

In the energy range below $10^{18.5}$ eV however, the SD trigger efficiencies are low as shown by the green dots in figure 4. In contrast, the red dots in this figure show that more than 90% EAS above $10^{17.0}$ eV make signals in at least one SD. To collect such small signals untriggered by the SD array itself we employed an external trigger of the SD array from the FDs called the hybrid trigger, because the trigger efficiency of the FD to such small EAS is higher than the SD trigger efficiency. For example, at $10^{18.0}$ eV the FD trigger efficiency is about 40%, it is about three times as high as the SD trigger efficiency at that energy.

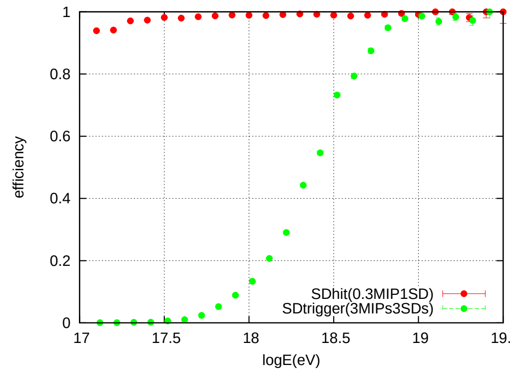

Figure 4: The simulation results of the SD trigger efficiencies and SD particle detection efficiencies.

Item	Criteria
search area	the nearest SD branch
time window	20us ±64us after FD trigger
threshold	0.3 MIP

Table 1: The SD signal selection criteria for hybrid trigger events. MIP means minimum ionizing particles.

2 Hybrid Trigger

The hybrid trigger operates as follows: First, when a FD station detects an EAS candidate, an external trigger is thrown from a PC (called FDPC) in the FD station to the nearest SD control PC (called SDPC) using TCP/IP. Upon receipt of this trigger, SDPC queues a request for collecting SD signals that fulfill the criteria shown in table 1. At the appropriate time, the SDPC sends that request to all of the SDs in its sub-array. It then collects any signals from the SDs in its sub-array, and sends its status back to FDPC. Finally the analysis is done off-line once the data from that day has been collected and written to an archive. To search for hybrid events easily, the SD and FD events are tagged using flags and time stamps.

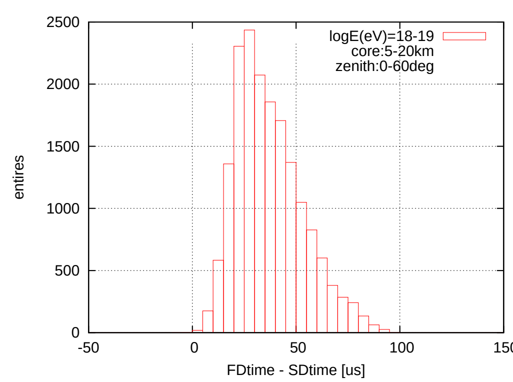

Figure 5: The simulation results of the clock timing difference between FD trigger timing and SD timing

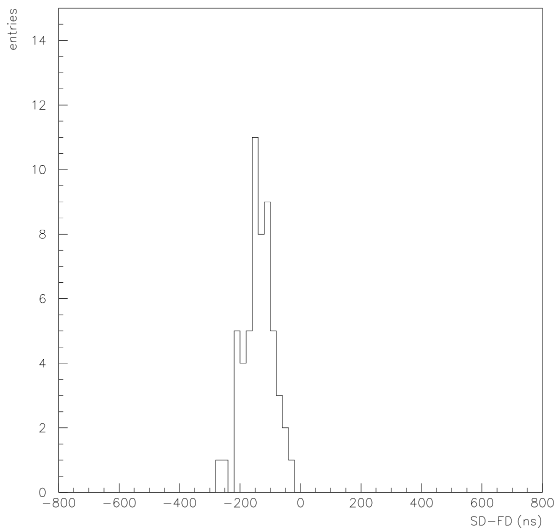

Figure 6: The measurement results of timing differences between SD and FD.

Before settling on the collection criteria in table 1, we studied how best to do this. For instance, we investigated timing and width of the SD search window. Figure 5 shows the results of the difference for simulated events between the trigger time as recorded by an FD station, and that by an SD. From this figure, we determined that the SD search window is centered about 20 usec after the FD trigger and its width is ±64 usec. With these criteria, 98.4% of simulated events are accepted.

The hybrid trigger rate is limited by the traffic capacity of a long distance wireless LAN. To reduced the hybrid trigger rate, events that are unlikely to be an EAS are removed by a filter program. The filter removes 99.99% of events such as atmospheric muon, chance coincidences from noises, calibration events, and other artificial lights from recorded FD events. It reduces the hybrid trigger to about 0.01 Hz from the normal FD trigger rate of about 2 Hz. From simulation studies, all triggered events above the energy 10^{18} eV are selected by this filter, only 20% of triggered events at 10^{17} eV are removed accidentally. The filtering process is done within 1 sec; there is no significant dead time increase in the FD data acquisition. In addition, signal latency is less than 1 sec including delay caused by collisions and retransmitting of packets. This is short compared with the SD signal buffering time of 16 sec.

3 Performance check

3.1 Timing differences between SD and FD

To use SD timing information in FD mono analysis, the difference the SD and FD clocks should be negligible, because EAS reconstruction strategies depend strongly on

date	hybrid trigger	BR station		
		SD response		
		timeout	SD self	waveform collected
Oct.08	76	0	1	75
09	84	0	2	82
10	72	0	3	69
11	93	0	5	88
12	83	0	2	81
13	61	0	2	59
14	75	0	1	74
15	43	0	1	42
16	27	0	0	27

Table 2: SD response for hybrid trigger in 2010 October. ”timeout” means that event collection was failed by timeout. ”SD self” means that signals were collected with SD trigger itself. ”waveform collected” means that signals were collected with hybrid trigger.

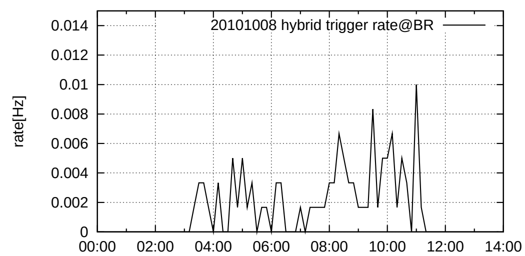

Figure 7: Hybrid trigger rate of BRM station on the first observation day (October 08, 2010).

timing. Each FD station and each SD has a clock that is adjusted using the GPS 1PPS signal [14, 13]. Previously, we determined that the time difference between two SDs is 20 nsec [13]. For this project, we investigated the difference between SD clock and FD clock using a vertical laser located at the center of the SD array called the CLF [15]. A small portion of the CLF vertical laser beam was guided to a PMT that was controlled by a set of SD electronics. Using this setup, we measured the timing of the laser shot at the CLF. The same beam was also seen by all the FD stations 20 km away. From the measured data at the FD, we estimated the laser timing at the roof of the CLF. Comparing the two timings showed that the difference was 150 nsec, as shown in Figure 6.

3.2 Operation status

We installed the hybrid trigger system at Black Rock Mesa (BRM) FD and Long Ridge (LR) FD in October 2010; the system has operated stably since that time. Table 2 shows the numbers of hybrid triggers and SD responses during the first week. The column labeled “Timeout” means the trigger request was delayed beyond the SD data buffering width of 16 sec. During this observation period, timeouts did not occur and all hybrid triggers were received by

month	BR branch		LR branch	
	SD self	hybrid trg	SD self	hybrid trg
Oct	18	136	15	124
Nov	18	141	22	146
Dec	22	249	29	342
total	58	526	66	612

Table 3: The number of events reconstructed using the data obtained from 2010 October to December. “SD self” and “hybrid trg” means the data taken by the SD self trigger and by hybrid trigger respectively.

the SDPC in time. The columns labeled “SD self” and “waveform collected” means that these events were collected with the SD trigger itself, or with the hybrid trigger, respectively. As shown in the table, all hybrid triggers were treated by the SDPC appropriately. Figure 7 shows the hybrid trigger rate from BRM FD to the BRM subarray on October 08, 2010. The maximum rate was 0.01 Hz on 11:00; that was caused by the filter letting LIDAR [16] pulses through to cause triggers. We improved the filter program to remove that contamination.

Presently we are checking the quality of the data collected by the hybrid trigger to see how well it helps to reconstruct EAS precisely. Preliminary results show that the use of the hybrid trigger provides ten times more reconstructable events than before as shown in table 3. This increased ratio is consistent with our expectations.

4 Summary

Installation of the hybrid trigger system at Black Rock Mesa FD and Long Ridge FD has been finished in October 2010; SD signals induced by smaller EASs are recorded during FD observation using hybrid trigger since that time. Use of SD signals improves the reconstruction accuracies of FD mono analysis in the lower energy range below $10^{18.5}$ eV. Using these observed data, we are studying arrival directions, energy spectrum, and composition at the lower energy range.

Acknowledgments

The Telescope Array experiment is supported by the Japan Society for the Promotion of Science through Grants-in-Aid for Scientific Research on Specially Promoted Research (21000002) “Extreme Phenomena in the Universe Explored by Highest Energy Cosmic Rays”, and the Inter-University Research Program of the Institute for Cosmic Ray Research; by the U.S. National Science Foundation awards PHY-0307098, PHY-0601915, PHY-0703893, PHY-0758342, and PHY-0848320 (Utah) and PHY-0649681 (Rutgers); by the National Research Foundation of Korea (2006-0050031, 2007-0056005, 2007-0093860, 2010-0011378, 2010-0028071, R32-10130); by the Russian Academy of Sciences, RFBR grants 10-02-01406a and 11-02-01528a (INR), IISN project No. 4.4509.10 and Belgian Science Policy under IUAP VI/11 (ULB). The foundations of Dr. Ezekiel R. and Edna Wattis Dumke, Willard L. Eccles and the George S. and Dolores Dore Eccles all helped with generous donations. The State of Utah supported the project through its Economic Development Board, and the University of Utah through the Office of the Vice President for Research. The experimental site became available through the cooperation of the Utah School and Institutional Trust Lands Administration (SITLA), U.S. Bureau of Land Management and the U.S. Air Force. We also wish to thank the people and the officials of Millard County, Utah, for their steadfast and warm support. We gratefully acknowledge the contributions from the technical staffs of our home institutions and the University of Utah Center for High Performance Computing (CHPC).

References

[1] H. Kawai et al., Nucl.Phys.B Proc.Suppl, 2008, **175-176**: 221-226
[2] H. Kawai et al., J.Phys.Soc.Jpn. Suppl. A , 2009, **78**: 108-113
[3] Y. Tameda et al., in these proceedings of ICRC2011
[4] R. U. Abbasi et al., Phys. Rev. Lett. 2010 **104**: 161101
[5] J. Abraham et al., Phys. Rev. Lett. 2010 **104**: 091101
[6] H. Tokuno et al., Astropart phys. 2008 **29**: 453
[7] S. P. Swordy et al., Astropart phys. 2002 **18**: 129-150
[8] T. Abu-Zayyad et al. ApJ 2001 **557**: 686
[9] D.J. Bird et al. Phys. Rev. Lett. 1993 **71**: 3401
[10] D.J. Bird et al. ApJ 1994 **424**: 491
[11] T. Nonaka et al., ICRC2009 proceedings http://icrc2009.uni.lodz.pl/proc/pdf/icrc0974.pdf
[12] D. Ikeda et al., in these proceedings of ICRC2011
[13] T. Nonaka et al., ICRC2007 proceedings, 2007 **5**: 1005
[14] Y. Tameda et al., NIM A 2009 **609**: 227
[15] T. Tomida et al., in these proceedings of ICRC2011
[16] T.A. Stroman et al., in these proceedings of ICRC2011